

CLINICAL INVESTIGATION

Benign Disease

PARENCHYMAL CELL PROLIFERATION IN CORONARY ARTERIES AFTER PERCUTANEOUS TRANSLUMINAL CORONARY ANGIOPLASTY: A HUMAN TISSUE BANK STUDY

JAY P. CIEZKI, M.D.,* URS O. HÄFELI, PH.D.,* PRISCILLA SONG,*
NANCY URANKAR-NAGY, M.T.(A.S.C.P.),^{||} NORMAN B. RATLIFF, M.D.,[†] LISA RYBICKI, M.S.,[‡]
KEVIN BRILL,* AND DOMINIK MEIER, M.S.[§]

The Departments of *Radiation Oncology, [†]Anatomic Pathology, [‡]Biostatistics and Epidemiology, and [§]Biomedical Engineering, The Cleveland Clinic Foundation, Cleveland, OH, USA; and ^{||}The Institute of Pathology, Case Western Reserve University, Cleveland, OH, USA

Purpose: Restenosis after percutaneous transluminal coronary angioplasty (PTCA) remains a limitation of this technique. Arterial wall cell proliferation is a component of restenosis preventable with intravascular brachytherapy. This study attempts to locate the sites of cellular proliferation after PTCA so as to aid the optimization of this therapy.

Methods and Materials: Autopsy records from January 1, 1985 through December 31, 1995 were reviewed, and 27 patients who received PTCA prior to death were identified who also had evidence of PTCA on histologic examination of the arterial sections. The sections were subjected to immunohistochemical staining for proliferating cell nuclear antigen (PCNA) to detect the proliferating cells in the arterial sections, followed by image analysis to determine the proliferative index (PI) of all regions and layers of the section.

Results: The PI did not differ significantly according to vessel region (plaque, plaque shoulder, or portion of vessel wall with lowest plaque burden), vessel layer (intima, media, adventitia), or evidence of prior PTCA. There was a trend toward a higher PI in young lesions.

Conclusion: Cell proliferation in the vascular wall after PTCA was found throughout the treated arterial section's axial plane, not only in the periluminal region. © 1999 Elsevier Science Inc.

Restenosis, Angioplasty, Brachytherapy, Immunohistochemistry, Autopsy.

INTRODUCTION

Intravascular brachytherapy as a preventative treatment for restenosis after transcatheter vascular intervention is gaining currency (1, 2). The success of this treatment has prompted its empiric application using several devices. These techniques are in the introductory phase, and further advances are likely to be characterized by better coverage of the treatment target(s). The honing of a brachytherapy procedure to precisely treat the perceived treatment target, as has been done in the treatment of early-stage prostate cancer, leads to improved efficacy and decreased toxicity (3, 4). It is reasonable to believe that similar results will be achieved with further development of intravascular brachytherapy techniques. The major hindrance to these advances is the definition of the treatment target(s).

The study of the cause(s) of restenosis is an area of evolving consensus. It is clear that cellular proliferation is at

least partly responsible (5). This is an important recognition, because ionizing radiation is well known to inhibit cellular proliferation in the clinical setting of keloid prophylaxis (6). This has led to the application of radiation in animal models of restenosis with promising results for restenosis prevention (7, 8). These preclinical studies have prompted clinical trials that also report encouraging results (1, 2, 9). Optimization of this technique may lead to even better results with new devices that are attuned to the biology and anatomy of the vascular lesions treated with PTCA. To this end, it seems that targeting the radiation to the proliferating cells should be a reasonable strategy. This report describes the location and intensity of the proliferation of parenchymal cells within the vascular wall of patients who have had PTCA prior to death, so as to aid such optimization.

Immunohistochemical staining for proliferating cell nuclear antigen (PCNA) is the method chosen for identifying the proliferating parenchymal cells. Traditional methods of

Reprint requests to: Jay P. Ciezki, M.D., Department of Radiation Oncology, The Cleveland Clinic Foundation, Cleveland, OH 44195. Tel: (216) 445-9465; Fax: (216) 444-5331; E-mail: ciezki@radonc.ccf.org

Acknowledgments—The authors would like to thank Steven N. Emancipator, M.D., of the Case Western Reserve University Institute of Pathology for assistance with immunohistochemistry.

Accepted for publication 15 June 1999.

visual evaluation are labor-intensive and prone to investigator bias (10). Computer-based image analysis utilizes consistent criteria to evaluate samples and is therefore reproducible, objective, and reliable, making it an increasingly important option in the evaluation of histological samples (11). Successful image analysis methods for determining proliferation indices in various types of tissue sections have been reported in the literature (10, 12–14). We employ similar methods to determine the endpoints of this investigation using computer-generated proliferation indices.

METHODS AND MATERIALS

Case acquisition

The autopsy records from January 1, 1985 to December 30, 1995 from The Cleveland Clinic Foundation were reviewed. Sixty-four patients with a history of PTCA were identified, and the microscope slides of the treated coronary artery sections were retrieved from the archives. All slides were reviewed for evidence of the PTCA, for example, vascular trauma (15) and 27 were culled for evaluation because they displayed the stigmata of PTCA. Re-cuts of the 27 arterial sections were subjected to immunohistochemical staining and image analysis.

Immunohistochemical staining

PCNA is a 36-kD protein that is highly conserved between species. PCNA functions as a cofactor for DNA polymerase delta in both S phase and in DNA synthesis associated with DNA damage repair mechanisms (16). The PCNA molecule has a half-life in excess of 20 h and may be detected in non-cycling cells such as those in G₀ phase or those fixed within one day of death. PCNA was therefore chosen to detect proliferating cells in these autopsy specimens because they were fixed within one day of death, and the resting cell division rate in human arteries is longer than five half-lives of PCNA; therefore, the resting proliferative rate will not affect the analysis.

Sections of artery were fixed in formalin, embedded in paraffin, and cut at 2 μ m. Slides were heated in a 60°C oven overnight, deparaffinized through xylene and graded alcohols, and quenched in 0.5% aqueous hydrogen peroxide. Sections were microwaved (850 W) for 10 min in 0.1 M citric acid buffer (pH 6), cooled, and washed in phosphate buffered saline (PBS, pH 7.4). Incubating with 1.5% normal goat serum (Vector Laboratories, Inc., Burlingame, CA) in PBS for 30 min at room temperature blocked nonspecific sites. Monoclonal (PC 10) mouse anti-human Proliferating Cell Nuclear Antigen (Dako, Carpinteria, CA) was applied at a dilution of 1:200 in diluted normal goat serum for 1 h at room temperature. The primary antibody was detected by the VECTASTAIN-ABC kit for mouse IgG (Vector Laboratories), which consists of a biotinylated secondary antibody and an avidin-biotin enzyme complex. Each of these reagents, prepared according to the manufacturer, was applied sequentially to sections for 30 min at room tempera-

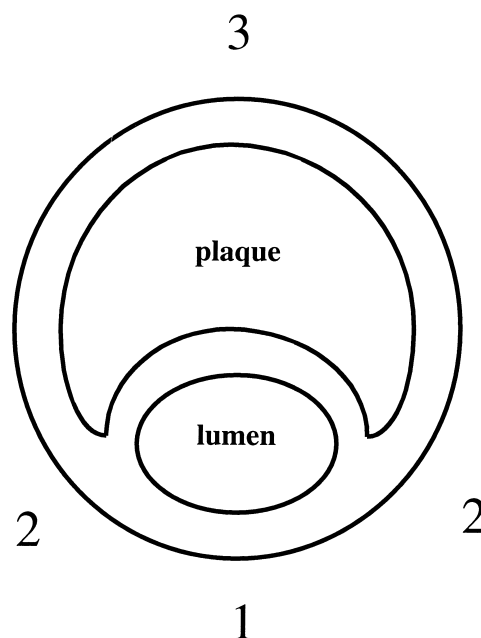


Fig. 1. Schematic of regions used for standardization of each arterial section. All sections were easily fitted to this schematic.

ture, washing in between with PBS. After a final wash, tissues were incubated with 3,3-diaminobenzidine tetrahydrochloride in hydrogen peroxide (Dako Liquid DAB) for 2 min, producing a reddish-brown precipitate. As controls, commercially prepared slides of human tonsil (Dako) were incubated with primary antibody and separately with PBS, and developed with the Vectastain Kit, under conditions identical to those employed with the sample sections.

Apparatus and images

For classification purposes, each arterial cross-section was subdivided into three regions corresponding to basic plaque morphology. As shown schematically in Fig. 1, the thickest region of the arterial wall (indicating the greatest area of neointima and/or plaque deposits) was designated as region 3, the thinnest region of the arterial wall was designated as region 1, and the regions of initial thickening separating regions 1 and 3 were designated as region 2.

Tissue sections were viewed in cross-section on a Nikon TMS light microscope. The images were captured using a DC-330 3CCD color video camera (Dage-MTI, Michigan City, IN) mounted on the microscope and a Flashpoint 128 video capture card (Integral Technologies, Indianapolis, IN). Four images each from the intima, media, and adventitia of each designated region were acquired, resulting in a total of 36 images for each tissue section. Thus, approximately 1.6 mm² of each arterial cross-section was captured for analysis. The color images were stored as uncompressed TIFF (tagged image file format) files in the RGB (red, green, blue) format.

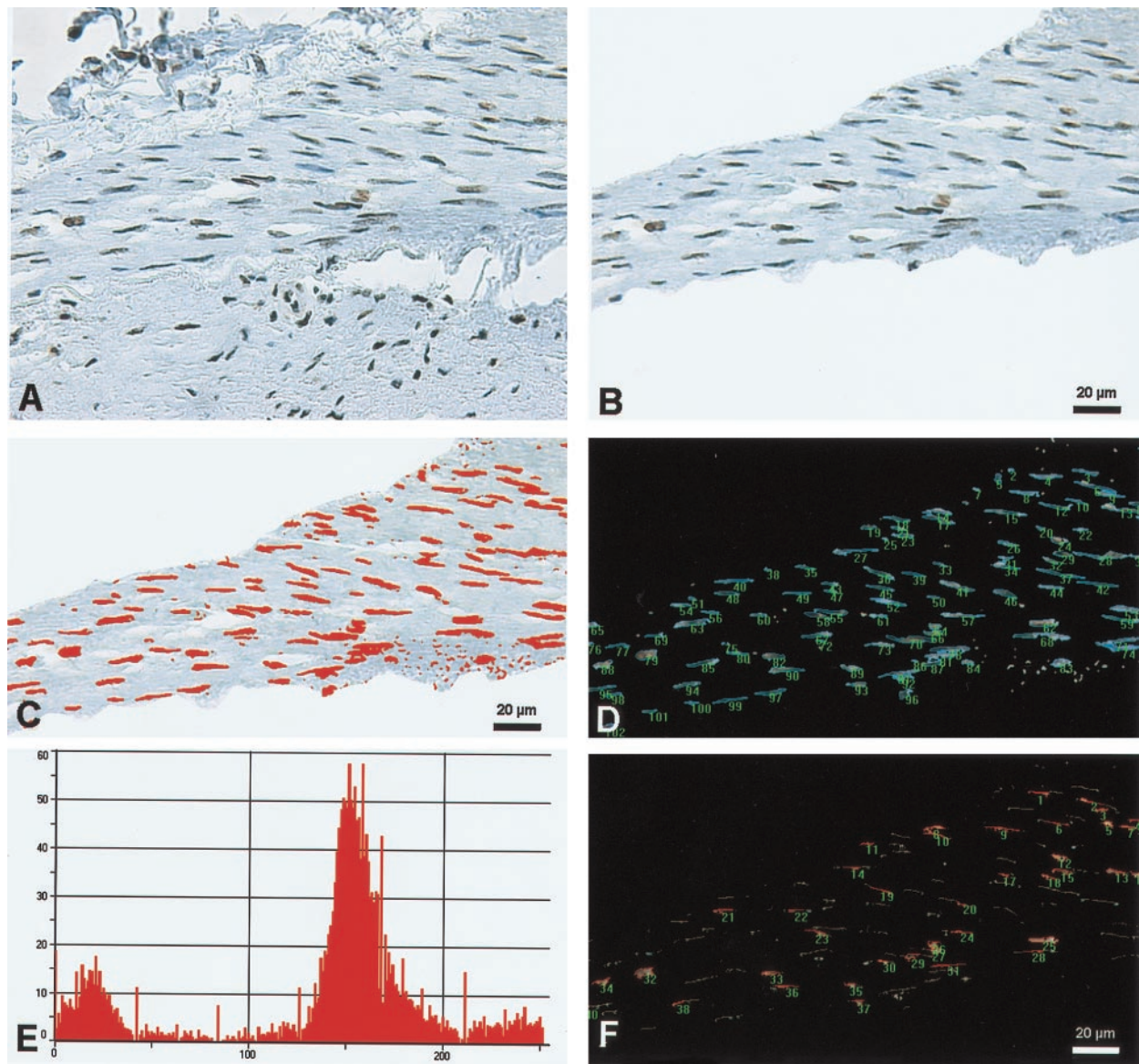


Fig. 2. (A) Original image of a representative arterial region immunohistochemically stained for PCNA (brown nuclei) and counterstained with hematoxylin (blue background) used for image analysis. (B) Isolation of the media of Fig. 2A for image analysis. (C) Interactive selection of an intensity threshold to establish a nuclear count. (D) Use of size threshold to discard non-nuclear material and then perform a total nuclear count. (E) Histogram of the 256 levels of hue identified in Fig. 2D. Those values of 0–42 and 213–255 correspond to brown, or the positive-labeling nuclei. (F) Numbered selection of the positive-labeling nuclei in Fig. 2D.

Initial image processing and rationale for using the HSI system

Images were processed and analyzed using the Image-Pro Plus image analysis program (Media Cybernetics, Silver Spring, MD) on a Pentium II personal computer. The original images captured by the video camera (an example is shown in Fig. 2A) were prepared for analysis. Next, the region of interest in each image was isolated, insuring that each image contained only a single designated region and a single arterial area (as shown in Fig. 2B).

The images were then transformed from the RGB color space to the HSI (hue, saturation, intensity) color space for

ease of analysis. In RGB color space, the separation of colors is dependent on the intensity; therefore, different colors may cluster closely together, making histogram-based segmentation difficult. In HSI color space, the brown and blue hues of the immunohistochemical staining were clearly separable in a 1-dimensional histogram, ultimately allowing the assessment of consistent proliferation indices of the arterial sections as explained below.

Image analysis

To establish the proliferation index of an artery section, the total number of nuclei and the number of positive-

Table 1. Descriptive statistics and test results comparing proliferation index among arterial layers and regions and according to prior intervention

Variable	*N	Mean	SD	Median	Minimum	Maximum	<i>p</i> -value
Region							
1	81	6.3	6.9	3.4	0.0	32.4	0.30
2	81	7.3	9.2	3.8	0.3	44.7	
3	81	6.4	7.8	3.6	0.0	35.8	
Layer							
Intima	81	5.9	6.3	3.8	0.0	32.4	0.11
Media	81	6.7	8.9	3.2	0.0	44.7	
Adventitia	81	7.5	8.6	3.8	0.4	37.0	
Prior intervention							
Yes	72	7.1	8.2	3.8	0.0	44.7	0.35
No	171	6.5	7.9	3.4	0.0	37.1	

* Number of microscopic fields subjected to image analysis.

labeling nuclei must be obtained. Both of these goals can be achieved by histogram-based clustering (thresholding), a widely used technique in image analysis that segments an image into relevant and irrelevant objects based on a pixel-wise classification scheme (17–19). We adapted the thresholding method described by Weaver and Au for human solid tumors to our present analysis of proliferation in artery sections (18). In brief, the method entails utilizing a threshold based on intensity information to establish the total number of nuclei. A second threshold makes use of the hue information to distinguish the positive nuclei from the negative nuclei.

Establishing the total number of nuclei

Interactive thresholding of the intensity spectrum of the HSI provided the required separation of the darker stained nuclei from the cytoplasmic background and cytoplasmic debris (see Fig. 2C). Spurious items such as non-nuclear structures or cellular debris were removed by masking the image with a size range corresponding to the expected nuclei. With both the intensity threshold and the size range applied to the image, a nuclear count was then performed. The result of these steps is demonstrated in Fig. 2D.

Determining the positive nuclei

Positive nuclei were indicated by the brown immunohistochemical staining (the result of the DAB chromagen recognition of the PCNA), while negative nuclei were distinguished by the blue hematoxylin counterstain. This distinction thus allowed us to utilize hue values to separate the positive nuclei from the negative nuclei. Hues representing positive nuclei are located in two clusters at the two ends of the hue spectrum and are separated by the blue hues of the negative nuclei (see Fig. 2E). The result of selecting the brown hue values is shown in Fig. 2F. Because the actual hue of the DAB chromagen was expected to remain relatively constant within the sample group (unlike the intensity of the staining which could be easily affected by variations in the staining environment), the same hue range was applied for all images in the study. The proliferative

index (PI) was calculated as the number of positive labeling nuclei/total number of nuclei; this was then multiplied by 100.

Statistical considerations

Two-factor repeated measures analysis was used to determine if the PI differed among layers or regions. The data were initially tested to determine if there was significant interaction between layers and regions. If interaction is not significant, then the PI can be compared among the three regions averaged across layers, or among the three layers averaged across regions. One-way analysis of variance with a repeated measures design was used to determine if the PI differed between lesions that underwent prior intervention and those which did not. Spearman's rank correlation coefficient was calculated to measure the association between PI and lesion age, separately for each region and layer. The correlation was tested to determine if it differed significantly from zero. All statistical tests were two-sided, and $p < 0.05$ was used to indicate statistical significance.

RESULTS

The median age (measured in days from time of the most recent intervention to time of death) of the lesions tested is 2 days (mean = 104.9, SD = 413.6, range of 0.1–2162). The majority (19 of 27) is less than 20 days old. Eight of 27 had at least one prior PTCA to the tested site. All sections were suitable for breakdown into the schematic seen in Fig. 1.

The primary endpoint of this analysis is locating the proliferating cells in the arterial wall. The PI did not differ between arterial regions 1, 2, and 3, arterial layers, or according to having a prior intervention (Table 1). Although the *p*-values are not significant, a trend was seen indicating the adventitia as a more active site of proliferation.

A statistically significant relationship of the lesion age with PI was not identified. However, it is noted that the sections in which PI was maximal are the younger sections of the series (Fig. 3).

REFERENCES

1. Teirstein P, Massullo V, Jani S, *et al.* Catheter-based radiotherapy to inhibit restenosis after coronary stenting. *N Engl J Med* 1997;336:1697–1703.
2. King SB III, Williams DO, Chougule P, *et al.* Endovascular β -radiation to reduce restenosis after coronary balloon angioplasty results of the beta energy restenosis trial (BERT). *Circulation* 1998;97:2025–2030.
3. Wallner K. An improved method for computerized tomography-planned transperineal iodine 125 prostate implants. *Oncology* 1991;5:115–122.
4. Ragde H, Elgamal AA, Snow P, *et al.* Ten-year disease free survival after transperineal sonography-guided iodine-125 brachytherapy with or without 45-gray external beam irradiation in the treatment of patients with clinically localized, low to high Gleason grade prostate carcinoma. *Cancer* 1998;83:989–1001.
5. Topol E, Serruys P. Frontiers in interventional cardiology. *Circulation* 1998;98:1802–1820.
6. Kovalic J, Perez C. Radiation therapy following keloidectomy: a 20-year experience. *Int J Radiat Oncol Biol Phys* 1989;17:77–80.
7. Waksman R, Robinson KA, Crocker IR, *et al.* Intracoronary radiation before stent implantation inhibits neointima formation in stented porcine coronary arteries. *Circulation* 1995;92:1383–1386.
8. Wiedermann JG, Marboe C, Schwartz A, *et al.* Intracoronary irradiation reduces restenosis after balloon angioplasty in a porcine model. *J Am Coll Cardiol* 1994;23:1491–1498.
9. Schopohl B, Liermann D, Pohlit LJ, *et al.* Ir-192 endovascular brachytherapy for avoidance of intimal hyperplasia after percutaneous transluminal angioplasty and stent implantation in peripheral vessels: 6 years of experience. *Int J Radiat Oncol Biol Phys* 1996;36:835–840.
10. Sallinen P, Haapasalo H, Kerttula T, *et al.* Sources of variation in the assessment of cell proliferation using proliferating cell nuclear antigen immunohistochemistry. *Anal Quant Cytol Histol* 1994;16:261–268.
11. Ong S, Jin X, Sinniah J, *et al.* Image analysis of tissue sections. *Comput Biol Med* 1996;26:269–279.
12. Lin H, Sotnikov A, Fosdick L, *et al.* Quantification of proliferating cell nuclear antigen in large intestinal crypt by computer-assisted image analysis. *Cancer Epidemiol Biomarker Prev* 1996;5:109–114.
13. Weaver J, Au J-S. Application of automatic thresholding in image analysis scoring of cells in human solid tumors labeled for proliferation markers. *Cytometry* 1997;29:128–135.
14. Ranefall P, Egevad L, Nordin B, *et al.* A new method for segmentation of colour images applied to immunohistochemically stained cell nuclei. *Anal Cell Pathol* 1997;15:145–156.
15. Gravanis M, Roubin G. Histopathologic phenomena at the site of percutaneous transluminal coronary angioplasty: The problem of restenosis. *Hum Pathol* 1989;20:477–485.
16. Yu C, Filipe M. Update on proliferation-associated antibodies applicable to formalin-fixed paraffin-embedded tissue and their clinical applications. *Histochem J* 1993;25:843–853.
17. Sahoo P, Soltani S, Wong K. A survey of thresholding techniques. *Comput Vision Graphics Image Process* 1988;41:233–260.
18. Weaver J, Au J-S. Comparative scoring by visual and image analysis of cells in human solid tumors labeled for proliferation markers. *Cytometry* 1997;27:189–199.
19. Russ J. The image processing handbook. Boca Raton: CRC Press; 1995.
20. Scott NA, Cipola GD, Ross CE, *et al.* Identification of a potential role for the adventitia in vascular lesion formation after balloon overstretch injury of porcine coronary arteries. *Circulation* 1996;93:2178–2187.
21. Teirstein P, Massullo V, Jani S, *et al.* A subgroup analysis of the Scripps coronary radiation to inhibit proliferation post-stenting trial. *Int J Radiat Oncol Biol Phys* 1998;42:1097–1104.
22. Malik N, Francis S, Holt C, *et al.* Apoptosis and cell proliferation after porcine coronary angioplasty. *Circulation* 1998;98:1657–1665.